Journal of Chromatography, 140 (1977) 187–195

CHROM. 10,209

CONVECTION IN CONTINUOUS-FLOW ELECTROPHORESIS

SIMON OSTRACH
Case Western Reserve University, Cleveland, Ohio (U.S.A.)
(Received April 4th, 1977)

SUMMARY

The various types of convection possible in an electrophoresis device are indicated and criteria are presented from which estimates can be made of the importance of convection in the separation. These criteria also indicate design options possible to suppress or reduce convection effects.

Specific consideration is then given to the convection induced by Joule heating in a representative continuous-flow electrophoresis configuration. Detailed solutions for the associated velocity and temperature distributions are presented and it is shown how they are influenced by the buffer through-put, wall cooling, and electric field intensity.

Significant distinction is pointed out between counter- and co-flow operation. With the latter mode it would appear that larger gap devices could be successfully run in a normal gravitational environment.

INTRODUCTION

The occurrence of natural convection in electrophoresis is thought to be detrimental because of the resulting mixing of the fluid. It is, therefore, important to establish criteria that will indicate under what conditions the convective flow will occur and what the nature of the flow is. Such information will indicate the design options available to eliminate or minimize such flows and how to scale meaningful models.

The basic configuration for continuous electrophoresis (see Fig. 1) is essentially a rectangular parallelopiped with the height, h, large relative to the width, w, and the depth, d. The ratio d/w is small also. The electrode length is denoted by L. In Fig. 1 the electrodes are shown located on the end walls; in some configurations they are placed on the side walls.

There are basically two modes of natural convection, *viz.*, conventional convection and unstable convection. These can occur separately or together in a given configuration. Conventional convection is generated immediately by a density gradient that is normal to the gravitational vector. Unstable convection can occur when the density gradient is parallel to but opposed to the gravity vector. The onset of this motion is not immediate but depends strongly on the geometry; once this motion

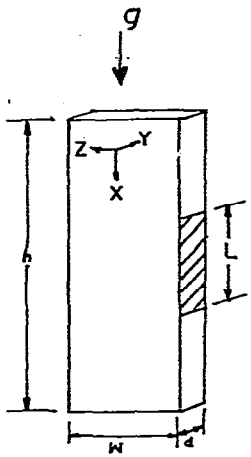

Fig. 1. Cell configuration.

starts, however, it causes much more mixing, in general, than conventional convection. Conventional convection, thus, results when the fluid and wall temperatures are different as with wall cooling and Joule heating. Furthermore, when the buffer flow is downward the fluid is heated as it proceeds along the cell. A vertical temperature (density) gradient, therefore, is imposed on the fluid with the higher temperature oc-

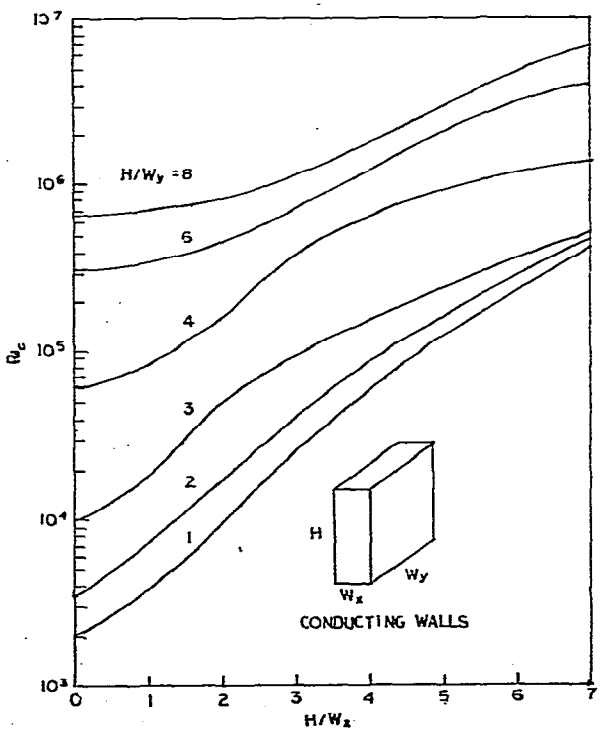

Fig. 2. Critical Rayleigh number as a function of aspect ratios (Catton[1]).

curring at the lower end of the cell, so that the heavier fluid is above the lighter. In such an unstable configuration no fluid motions are induced until a critical temperature (density) gradient, or non-dimensionally, a Rayleigh number is exceeded; this critical value depends on the fluid properties but, more importantly, on the geometric configuration. The relation of the critical Rayleigh number with the two aspect ratios of significance for the configuration of interest herein is presented in Fig. 2 to (ref. 1).

From the above it should be evident that both types of convection are possible in a continuous-flow electrophoresis cell. One may dominate the other depending on the design and operating conditions. Thus, it is necessary to make estimates for each type of convection.

CONVECTION CRITERIA

In order to obtain some quantitative results let us assume that a representative configuration has $h = 30.5$ cm, $w = 5.08$ cm, $d = 0.508$ cm, and $L = 10.16$ cm. Let us also assume that the buffer properties are similar to water so that the kinematic viscosity, $\nu = 1.4 \times 10^{-2}$ cm^2/sec, the volumetric expansion coefficient $\beta = 0.18 \times 10^{-3}$ °K^{-1}, the thermal conductivity, $k = 0.56$ W/m °K, and the Prandtl number $Pr = 10$.

Convectional convection

The dimensionless parameter that indicates the ratio of buoyancy to viscous forces[2] is the Grashof number, $Gr = \beta g \Delta T l^3/\nu^2$ where g is the gravitational force, ΔT denotes a characteristic temperature difference, and l a characteristic length. For the specific example being considered the difference in temperature between the fluid and the wall is taken to be 5 °K and the characteristic length $l = d/2 = 0.254$ cm so that $Gr = 73.8$. An estimate of the velocities induced under these conditions can be made from

$$u = \sqrt{Gr}\,(2\nu/d) = \sqrt{\beta g \Delta T (d/2)} = 0.472 \text{ cm/sec.}$$

From this expression it is clear that the most convenient design option to reduce convection is to reduce the characteristic length.

Unstable convection

The parameter that determines the onset of unstable convection[2] is the Rayleigh number.

$$Ra_c = Pr\, Gr_c = Pr \frac{g \Delta \varrho_c L^3}{\varrho \nu^2} = \frac{\beta g \Delta T_c L^3}{\nu^2}$$

where $\Delta\varrho$ is a characteristic density difference and the subscript c denotes the critical condition. For the cell in the vertical orientation $h/d = H/W_x = 60$, $h/w = H/W_y = 6$. For these conditions it can be estimated from Fig. 2 that $Ra_c = 2 \times 10^6$. With $L = 10.16$ cm the critical temperature difference can be determined from

$$\Delta T_c = 2 \times 10^6 \frac{\nu^2}{Pr \beta L^3 g} = 0.214 \text{ °K}$$

A difference in temperature (from bottom to top) greater than this value will lead to unstable convection.

If the cell is placed horizontally on the large side walls the configuration simulates an unbounded horizontal fluid layer half of which is heated from below. The critical Rayleigh number for such a situation[3] is 1101. Thus the characteristic length is $d/2 = 0.254$ cm and the critical temperature difference is $\Delta T_c = 7.5$ °K. The considerable stabilization obtained from a simple change in cell orientation is obvious. However, in this configuration conventional convection would result because the horizontal temperature difference is normal to the vertical gravity vector.

It must be noted that the values of the critical Rayleigh numbers have been determined for situations where all fluid motions are due solely to gravitational effects. It has been shown that, for proper conditions, superposed co-flows do not alter the critical Rayleigh numbers. However, for counter-flows such as would result with downward buffer flow there is no information.

Combined force and natural convection

In continuous-flow electrophoresis the fluid motions generated by buoyancy occur simultaneously with the forced flow of the buffer. The importance of the buoyancy-induced motions relative to the forced ones can be estimated[2] from the ratio of the Grashof and square of the Reynolds numbers:

$$\frac{Gr}{Re^2} = \frac{\text{buoyancy force}}{\text{inertia force}} = \frac{g\Delta\varrho l^3}{\varrho\nu^2}\left(\frac{\nu^2}{U^2 l^2}\right) = \frac{g\Delta\varrho l}{\varrho U^2}$$

where U is the buffer velocity. Convection will be negligible if

$$\frac{g\Delta\varrho l}{\varrho U^2} \ll 1$$

This inequality indicates the design options possible to minimize or eliminate the effects of natural convection is a combined flow field.

It must be emphasized that the criteria given above are useful to obtain qualitative and order-of-magnitude estimates. Some of the variables used above could be written in terms of others, *e.g.*, ΔT could be expressed in terms of the electrical power used. Also, in applying them all coupling mechanisms must be kept in mind. For example, from the last inequality presented above one might think that all convection problems could be avoided by increasing the buffer velocity. However, the sample residence time would be reduced accordingly and that trade-off would have to be considered.

CONVECTION INDUCED BY JOULE HEATING

Order-of-magnitude estimates are useful but it would be of interest to examine some details now. Let us, therefore, find the velocity and temperature distributions in the buffer generated by Joule heating. To this end consider the fully developed flow of a quasi-incompressible viscous fluid in a channel like that shown in Fig. 1. The wall temperatures are taken to be constant and equal because of wall cooling and an

electric current through the fluid causes Joule heating. The analysis of ref. 4 can easily be modified to the present case to yield

$$\theta = \theta_w + \frac{\sigma E^2 l^2}{2k}[1 - (Y/l)^2] \tag{1}$$

$$u = \frac{l^2[1 - (Y/l)^2]}{2\mu}\left\{-\frac{dP}{dX} - \varrho\beta g\theta_w - \frac{5}{12}\frac{\varrho\beta g\sigma E^2 l^2}{k}\left[1 - \frac{(Y/l)^2}{5}\right]\right\} \tag{2}$$

where $\theta = T - T_s$ is the temperature difference, T_s is a reference temperature (here, the buffer temperature before it enters the electric field), θ_w is the wall temperature difference, σ is the electric conductivity, E is the electric field intensity, l half the gap distance ($d/2$), μ the absolute viscosity and P the pressure. Note these solutions (with a coordinate stretching) are applicable to fluids with variable viscosities and thermal conductivities.

From eqns. 1 and 2 it can be seen how each of the design and operating conditions influence the velocity and temperature profiles. For example, the factor of the last term of eqn. 1 equals the difference between the maximum fluid temperature and the wall temperature due to Joule heating. In eqn. 2 the first term on the right can be directly related to the buffer through-put, the second term is due to wall cooling, and the last to Joule heating. Note that the signs in the above equations correspond to the coordinate system indicated on Fig. 1; in particular X increases downward.

It is essential to understand that the buffer and sample flows can be directed in the direction of the gravity vector (downward) or opposed to it (upward). The former is the one usually considered although a few devices actually operate in the latter fashion. If the buffer flow is downward the first and third terms in eqn. 2 are of opposite signs (dP/dX is negative) which indicates that the convective flow induced by Joule heating opposes the downward buffer flow. The sign of the second term is determined by $T_w - T_s$ which for cooled walls is negative so that the second term is positive and, thus, enhances the first term. If, however, the buffer flow is directed upwards the first and third terms are both negative so that Joule heating enhances the buffer flow. Thus, the direction of the buffer flow (or orientation of the device) profoundly influences the resultant flow. For downward buffer flows the convection opposes it and can ultimately destroy the parabolic profile. The convection will reinforce upward buffer flows so that the velocity profile will always be parabolic with different scales, *i.e.*, the flow is cocurrent.

The buffer volume flow-rate, Q^*, can be related to the pressure gradient as[5]

$$-\frac{1}{\mu}\frac{dP}{dX} = \frac{2}{3}\frac{Q^*}{wl^3}$$

so that eqn. 2 can be written as

$$u = \frac{l^2[1 - (Y/l)^2]}{2\mu}\left\{\frac{2}{3}\frac{Q^*}{wl^3} - \varrho\beta g\theta_w - \frac{5}{12}\frac{\varrho\beta g\sigma E^2 l^2}{k}\left[1 - \frac{(Y/l)^2}{5}\right]\right\} \tag{2a}$$

From this equation it is obvious that a reduced-gravity environment would reduce the Joule heating effect. However, it will be useful to investigate the conditions under

which the Joule heating will be detrimental in general for downward buffer flows ($Q^* > 0$).

The velocity distribution can now be seen to take on different shapes depending on the relative magnitudes of the design variables. Thus, if

$$\frac{2}{3}\frac{Q^*}{wl^3} \geqslant \frac{\varrho\beta g}{\mu}\left[\theta_w + \frac{\sigma E^2 l^2}{2k}\right] \tag{3}$$

the profile is a parabola as in Fig. 3a. If, however,

$$\frac{\varrho\beta g}{\mu}\left(\theta_w + \frac{5}{6}\frac{\sigma E^2 l^2}{2k}\right) < \frac{2}{3}\frac{Q^*}{wl^3} < \frac{\varrho\beta g}{\mu}\left(\theta_w + \frac{\sigma E^2 l^2}{2k}\right) \tag{4}$$

the flow in the vicinity of the axis (along which the sample flows) is retarded as in Fig. 3b. Finally, if

$$\frac{2}{3}\frac{Q^*}{wl^3} < \frac{\varrho\beta g}{\mu}\left(\theta_w + \frac{5}{6}\frac{\sigma E^2 l^2}{2k}\right)$$

the velocity near the axis will actually be reversed as shown in Fig. 3c.

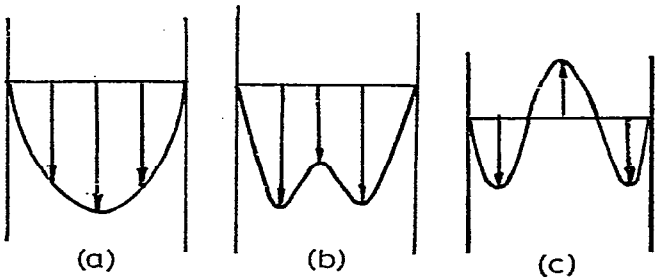

Fig. 3. Velocity profiles. a, Parabolic profile; b, retarded profile; c, reversed profile.

An estimate of the relative magnitudes of velocities induced by buoyancy (due either to wall cooling or Joule heating) can be made by comparing the corresponding terms of eqn. 2 evaluated at the channel axis ($Y = 0$). Thus, for example, the velocities induced by Joule heating compared to the buffer average velocity, U is

$$\frac{u_J}{U} = \frac{5}{24}\frac{\varrho\beta g\sigma E^2 l^4}{\mu k U} = \frac{5}{24}\frac{Gr_J}{Re} \tag{5}$$

where $Gr_J = \dfrac{\beta g\sigma E^2 l^2}{\nu^2}$ and $Re = U \cdot l/\nu$.

Again design options to reduce the convective effects are indicated in eqn. 5.

A separate analysis was made to determine the factors that influence the separation of a particle in a flow field with an electric field. To that end the trajectory was determined of a particle with a diameter d_i having a charge q_i subject to a Stokes drag

force and an electric field. Diffusion effects were neglected. It was found that the ratio of the maximum distance normal to the flow direction to the length of flow D is

$$\frac{X_{max.}}{D} = \frac{q_i E}{3\pi\mu d_i v_f} \tag{6}$$

where v_f is the fluid velocity due both to the forced and natural-convection flows. Eqn. 6 is, in effect, a measure of the resolution and the factors that influence it are indicated therein. This equation is strictly valid only for thick double layers. For thin double layers which are more likely in the electrophoresis of biological materials the right side of eqn. 6 contains a small factor (inversely proportional to the Debye length) due to electrokinetic streaming[6]. It can be observed that it would be beneficial to reduce the fluid velocity to improve resolution. That could, of course, be done by reducing the buffer flow.

SPECIFIC EXAMPLES

The general considerations treated above will now be applied to two specific continuous-flow electrophoresis devices: one representative of those currently used for analysis and one proposed to operate with considerably greater through-put in space. They will be referred to herein as the ground-based apparatus and the space flight apparatus. Representative values for the buffer properties are: $\sigma = 7.3 \times 10^{-4}$ mho/cm, $\beta = 0.18 \times 10^{-3}$ °K^{-1}, k = 0.5 W/m °K, and $\nu = 1.4 \times 10^{-2}$ cm^2/sec.

Ground-based apparatus

For this device the following representative values will be used: $g = 980$ cm/sec^2, $E = 86$ V/cm, $l = 0.075$ cm, $w = 7$ cm, and $L = 45$ cm. To determine the maximum temperature rise in the buffer due to Joule heating eqn. 1 is evaluated at the axis ($Y = 0$) to yield:

$$\theta_{max.} - \theta_w = T_{max.} - T_w = \frac{\sigma E^2 l^2}{2k}$$

so that for the values given above $T_{max.} - T_w = 2.76$ °C. The Grashof number, which represents the ratio of buoyancy to viscous forces, is

$$Gr = \frac{\beta g (T_{max.} - T_w) l^3}{\nu^2} = 1.03$$

This indicates that the flow will be relatively slow and laminar. Evaluation of all the terms in eqn. 2a with $Q^* = 15$ cm^3/min $= 0.25$ cm^3/sec indicates that even with buffer downflow the velocity profile will be parabolic, *i.e.*, the first term is dominant. Thus, the maximum velocity (at the axis, $Y = 0$) is

$$u_{max.} = \frac{l^2}{2}\left[\frac{2Q^*}{3wl^3} - \frac{\beta g\theta w}{\nu} - \frac{5}{12}\frac{\beta g\sigma E^2 l^2}{k\nu}\right] = 0.15 \text{ cm/sec}$$

with $\theta_w = -2$ °C. Note that estimating the velocity from the expression $u = \sqrt{Gr}(\nu/l)$ presented in the section Convection criteria yields a value of 0.189 cm/sec. For the given electrode length, $L = 45$ cm, the residence time, τ, is

$$\tau = L/u_{\max.} = 300 \text{ sec}$$

If, on the other hand, the buffer flow were upward, $u_{\max.} = 0.168$ cm/sec and $\tau = 268$. In view of the previous discussion concerning the differences with downward and upward buffer flows it can be seen that in the former case the Joule heating results in a lower maximum velocity and, therefore, leads to a greater residence time whereas the reverse is true for upward buffer flow which is increased by the Joule heating.

Increases in the electric field intensity will ultimately modify the parabolic velocity profile with downward buffer flow. However, the field intensity can be increased with upward buffer flow. The residence time may be reduced by such increases but the electrode length can be increased to compensate for this. With upward buffer flow the field intensity increases is limited only by the maximum fluid temperature difference permissible for the particular biological samples. For the specific conditions treated herein and for $(T_{\max.} - T_w) = 5$ °C, the maximum field intensity could be 117 V/cm. Even with this field intensity the residence time would still be approximately 200 sec.

Space-flight apparatus

Since greater through-put is desired for this device the gap width is increased to 0.5 cm so that $l = 0.25$ cm. Also $w = 5$ cm, $L = 10$ cm, and $E = 69$ V/cm. All other values are the same as previously used. Thus, it is found that $(T_{\max.} - T_w) = 19.4$ °C and the Grashof number is 273 based on the earth's gravity ($g = 980$ cm/sec^2). Such a low value for Gr implies that the convection will be laminar and relatively slow and would not ordinarily be detrimental. However, the difficulty arises from the counterflow. The velocity profile determined from the specified values for this case and eqn. 2a for downward buffer flow is a reversed-flow one like that in Fig. 3c and this would, therefore, be unacceptable. If the buffer flow were upward a parabolic profile would be obtained. However, the velocities would be so large that the residence time would be too short. To compensate for this the electrode length would have to be increased. Clearly, these difficulties could be overcome for both orientations in a space vehicle where the gravitational force is reduced by five or six orders of magnitude. (Note that g is in the numerator of the Joule heating term in eqn. 2.) However, the analysis has indicated a number of design options that could permit the apparatus to be designed with the large gap and to operate on earth. This would require a decrease in field intensity and an increase in the electrode length with possibly a reduction in residence time. For example, if a residence time of 100 sec were acceptable an increase in the electrode length to 100 cm and a decrease in field intensity to 27 V/cm would then permit operation of the wider-gap device on earth. Other trade-offs are, of course, possible. From the relations presented herein design or operating charts can be developed that relate the electric field intensity, maximum temperature difference, gap width, residence time, electrode length, and buffer flow-rate in order to indicate the trade-offs explicitly. These would also indicate the bounds within which large-gap devices could operate in a normal gravitational environment.

SUMMARY

A number of criteria are presented that permit estimates to be made of various convective effects on continuous-flow electrophoresis. Design options possible to eliminate or reduce these effects are indicated therefrom. The detailed velocity and temperature distributions are then presented as functions of the buffer flow-rate, wall cooling, and Joule heating. Several different flow regimes are delineated in this way and the significant differences between counterflow and co-flow operation are indicated. In particular, it is shown that it appears possible to operate a large-gap device in a normal gravitational environment if the buffer flow is upward (co-flow). It should also be mentioned that with upward buffer flow the possibility of a thermal instability due to heating from below need not occur (with proper design) because the heated (electrode) region overlays the region of incoming cool buffer flow. Thus, the upward buffer flow configuration seems to be free of at least two possible causes of remixing. Such a configuration has been utilized to separate simple dyes[7,8].

The emphasis throughout the present paper is to gain some understanding of the relevant phenomena in order to make clear the design options. Other hydrodynamic aspects (such as electro-osmosis, stream stability, Taylor dispersion, and sample concentration) of continuous flow electrophoresis need to be investigated in greater detail so that proper design can be made of such devices for preparative purposes.

REFERENCES

1 I. Catton, *J. Heat Transfer*, 94 (1972) 446.
2 S. Ostrach, *Laminar Flows with Body Forces, High Speed Aerodynamics and Jet Propulsion, Vol. 4, Theory of Laminar Flows*, Princeton Univ. Press, Princeton, 1964.
3 A. Pellew and R. V. Southwell, *Proc. Roy. Soc. London*, A176 (1940) 312.
4 S. Ostrach, *Laminar Natural-Convection Flow and Heat Transfer of Fluids with and without Heat Sources in Channels with Constant Wall Temperatures*, National Advisory Committee for Aeronautics, Washington, D.C., 1952.
5 R. H. Sabersky, A. J. Acosta and E. G. Hauptmann, *Fluid Flow: A First Course in Fluid Mechanics*, Macmillan, New York, 2nd ed., 1971, p. 57.
6 D. A. Saville, *Annu. Rev. Fluid Mech.*, 9 (1977) 321.
7 R. Dobry and R. K. Finn, *Science*, 127 (1958) 697.
8 R. Dobry and R. K. Finn, *Chem. Eng. Progr.*, 54, No. 4 (1958) 59.